

# Highly Porous (TiO<sub>2</sub>–SiO<sub>2</sub>–TeO<sub>2</sub>)/Al<sub>2</sub>O<sub>3</sub>/TiO<sub>2</sub> Composite Nanostructures on Glass with Enhanced Photocatalysis Fabricated by Anodization and Sol–Gel Process

Song-Zhu Chu,\* Satoru Inoue, Kenji Wada, Di Li, Hajime Haneda, and Satoshi Awatsu

Advanced Materials Laboratory, National Institute for Materials Science (NIMS), Namiki 1-1, Tsukuba, Ibaraki, 305-0044, Japan

Received: April 10, 2003

Three-dimensional highly porous TiO<sub>2</sub>–4%SiO<sub>2</sub>–1%TeO<sub>2</sub>/Al<sub>2</sub>O<sub>3</sub>/TiO<sub>2</sub> composite nanostructures ( $\phi$ 30–120 nm) directly fixed on glass substrates were fabricated by anodization of a superimposed Al/Ti layer sputter-deposited on glass and a sol–gel process. The porous composite nanostructures exhibited enhanced photocatalytic performances in decomposing acetaldehyde gas under UV illumination, which can be mainly ascribed to the combination of their large surface areas (7750–14770 m<sup>2</sup>/m<sup>2</sup>), high porosities (34.2–45.6%), and transparency. Specially, the composite nanostructure with  $\sim\phi$ 120 nm pores calcined at 500 °C showed the highest photocatalytic activity that is 6–10 times higher than commercial P-25 TiO<sub>2</sub> under the experimental conditions.

Titanium dioxide has attracted much attention in the field of photocatalytic application for environmental purification, decomposition of harmful substances, and utilization of solar energy.<sup>1–12</sup> To acquire high photocatalysis in decomposing various harmful substances in gas or liquid, TiO<sub>2</sub> materials need to be fabricated with high specific surface areas and highly porous structures (preferred in nanoscale) for effective contact with reactant substances. So far, extensive studies have been done to achieve various TiO<sub>2</sub> nanomaterials with large surface areas (powder,<sup>2–4</sup> nanotubes,<sup>5–9</sup> nanofibers,<sup>10</sup> thin films comprised of nanocrystals<sup>11,12</sup>) by many methods such as sol–gel process,<sup>3,5–9</sup> pulsed laser deposition,<sup>10</sup> and electrodeposition.<sup>11,12</sup> Specially, the nanostructured TiO<sub>2</sub> materials (nanotubes and nanofibers), which are fabricated through a template-synthesis method that was pioneered by Martin's group,<sup>5–7</sup> have attracted much interest in this decade because of the large surface areas and various potential applications of the materials. In the template-synthesis method, commercial porous alumina membranes ( $\phi$ 22 or  $\phi$ 200 nm, several centimeters in diameter and 50–100  $\mu$ m thick) were used as templates in a sol–gel process. After removing the alumina templates, nanotube-shaped TiO<sub>2</sub> powder<sup>8,10</sup> and/or bush-like TiO<sub>2</sub> nanotubes or nanofibers arrays<sup>5–7</sup> were obtained. Several potential applications of the TiO<sub>2</sub> nanostructures were investigated, including as photocatalyst.<sup>7</sup> Nevertheless, from the viewpoint of practical applications, exploring a nanostructured TiO<sub>2</sub> material with high photocatalytic performance and improved mechanical strength is vital and still remains a challenge for scientists.

Our work aims to fabricate a nanostructured TiO<sub>2</sub>-based material directly on glass to achieve enhanced photocatalysis and mechanical strength. In our previous studies,<sup>13,14</sup> we described the fabrication of transparent TiO<sub>2</sub> nanotubule arrays on ITO/glass substrates by Al anodization and sol–gel process. The porous alumina films on glass formed by anodizing sputter-deposited Al layers were performed as templates in the successive sol–gel process. In this paper, we report an improved route to fabricate highly porous TiO<sub>2</sub>–SiO<sub>2</sub>–TeO<sub>2</sub>/Al<sub>2</sub>O<sub>3</sub>/TiO<sub>2</sub>

composite nanostructures on Ti/glass substrates. Here the porous alumina films are used as a carrier material and are remained to acquire necessary mechanical strength. The porosity and pore dimensions of the anodic alumina nanostructures can be readily controlled by adjusting the anodizing conditions (solution, voltage or current) and the successive pore-widening time.<sup>13,15–17</sup> So can the final surface areas of nanostructures be further adjusted and enhanced by the successive sol–gel coating. Moreover, to confirm the enhancement on photocatalysis, the photocatalytic performances of the resultant nanostructures were also investigated by decomposing acetaldehyde gas under UV illumination.

The starting sample was a superimposed aluminum (99.99%,  $\sim$ 1.5  $\mu$ m)/titanium (99.99%,  $\sim$ 200 nm) layer deposited successively on a glass substrate (soda lime glass, 25  $\times$  80  $\times$  1.1 mm) by a RF sputtering at a rate of 1.5 nm/s in a one-cycle mode. The anodization was performed in two steps: i.e., the specimens were first anodized potentiostatically in a 10 vol % phosphoric (110 V, 10 °C) or a 3 wt % oxalic (40 V, 20 °C) acid solution until the anodic current tends to  $\sim$ 5 A/m<sup>2</sup>, and then further anodized in a constant current mode at that value up to 150 V. The first step is to achieve a porous alumina nanostructure and the second step is to obtain a dense titania layer between the anodic alumina and the titanium layer. In sol–gel process, the anodized specimens were first immersed in a 5% (vol) phosphoric acid solution at 30 °C for 20 or 40 min to widen the pores and then dip-coated in a 2.5 wt % (TiO<sub>2</sub>–4%SiO<sub>2</sub>–1%TeO<sub>2</sub>) solution, followed by calcinations at 400–600 °C for 2 h for the crystallization of TiO<sub>2</sub>. Details on the synthesis of the sol and the conditions of sol–gel coating were described in a previous study.<sup>13</sup>

Figure 1 show the TST/Al<sub>2</sub>O<sub>3</sub>/TiO<sub>2</sub> composite nanostructures on glass synthesized upon phosphoric-anodized films (denoted as PF, left side) and oxalic-anodized films (denoted as CF, right side). The composite nanostructures comprise numerous open pores that distribute uniformly on the surface irrespective of the large roughness, even though some of the pores in the CF specimens are covered by the calcined TST layer (arrow in Figure 1b). Because of the induction of aluminum crystal grains

\* To whom correspondence should be addressed. Tel: +81-29-851-3354 (ext. 8600). Fax: +81-29-854-9060. E-mail: CHU.Songzhu@nims.go.jp.

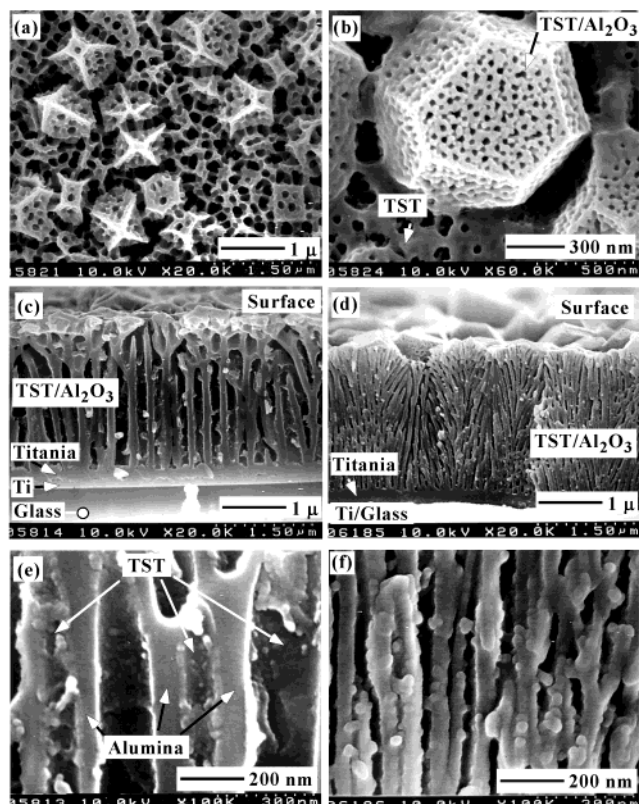


**Figure 1.** FESEM images of (a, b) surface morphologies and (c–f) fracture sections of porous TiO<sub>2</sub>–4%SiO<sub>2</sub>–1%TeO<sub>2</sub>/Al<sub>2</sub>O<sub>3</sub> composite nanostructures on glass substrates after being heated at 500 °C for 2 h. Left side, PF specimens anodized in 10% H<sub>3</sub>PO<sub>4</sub> and pore-widened for 40 min; right side, CF specimens anodized in 3% (COOH)<sub>2</sub> and pore-widened for 20 min.

during anodization,<sup>18</sup> a porous alumina with coral-like structure is formed (Figure 1c,d), leading to high porosities or large surface areas. From the high-resolution images (Figure 1e,f), it is seen that the TST adhered to the alumina walls and form a hollow structure. The TST layers (~20 nm for the PF and ~10 nm for the CF specimens) are continuous within the channels and exhibit a rough inner surface, thus leading to large surface areas that are not comparable for other conventional filmy TiO<sub>2</sub> materials. Here, that we have adopted a composite TiO<sub>2</sub>–4%SiO<sub>2</sub>–1%TeO<sub>2</sub> sol instead of a pure TiO<sub>2</sub> sol in the sol–gel coating is because the latter tends to form a granular TiO<sub>2</sub> layer that usually covers the apertures or blocks the channels of the porous alumina. The addition of SiO<sub>2</sub> and TeO<sub>2</sub> improves the wetting ability of TiO<sub>2</sub> sol and the affinity of the calcined layer to the anodic alumina walls, leading to a hollow composite structure with open apertures. It should be mentioned that the appropriate concentration (i.e., 2.5%) of the TST sol is also a very important prerequisite to acquire a hollow structure with open apertures. A thicker TST sol leads to the coverage of pores on alumina films, and a thinner sol usually produces a discontinuous layer or separate particles within the nanopores. Moreover, on the basis of the calculation from the FESEM images by a simulated program, the average porosities of the composite nanostructures are estimated to be ~45.6% and ~34.2% for the PF and the CF specimens, respectively. In addition, because the titanium layer is partly oxidized into a dense titania layer in anodization, a joined alumina–titania structure is formed on the Ti/glass substrate (Figures 1c and 1d). The anodic titania may work as a binding layer and provides a good adherence between the porous nanostructures and the glass substrates. The resultant composite nanostructures exhib-

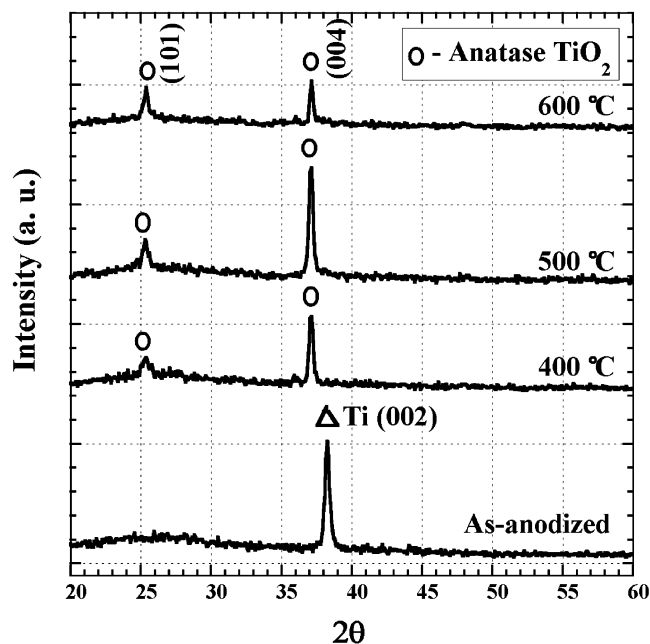


**Figure 2.** X-ray diffraction patterns of as-anodized alumina–titania/Ti/glass and porous TiO<sub>2</sub>–4%SiO<sub>2</sub>–1%TeO<sub>2</sub>/Al<sub>2</sub>O<sub>3</sub> composite nanostructures on Ti/glass obtained by sol–gel coating and heating at different temperatures. Anodization, 5% H<sub>3</sub>PO<sub>4</sub>; pore-widening, 40 min.

ited good adherence to the substrates in a mechanical peel-off test. No cracking or exfoliating phenomenon was found when cutting or breaking the specimens, indicating that it may be durable for various mechanical finishing.

X-ray diffraction (XRD) studies were carried out at different temperatures to investigate the crystallization of the anatase TiO<sub>2</sub> phase, which is the necessary structure for photocatalysis. The XRD patterns for the TST/Al<sub>2</sub>O<sub>3</sub>/TiO<sub>2</sub> composite nanostructures show two reflections at  $2\theta = 25.3^\circ$  and  $37.1^\circ$  which are assigned to anatase ( $d_{101}$  and  $d_{004}$ ). The {101} reflection becomes prominent with increasing temperature, whereas the {004} reflection is of the most prominent at 500 °C. For comparison, a XRD pattern for as-anodized specimen is also given in Figure 2. Only one reflection at  $2\theta = 38.3^\circ$  appears, which is identified to titanium ( $d_{002}$ ). Here, the composite nanostructures exhibit a preferential {004} reflection that is different from the flat TiO<sub>2</sub> film with a preferential {101} reflection.<sup>13</sup> This may be ascribed to the crystallization of the anodic titania layer (~200 nm) and/or the oxidation of the underlying titanium layer on glass substrate.

Figure 3 shows the nitrogen adsorption–desorption isotherms for the PF (~ $\phi$ 120 nm) and CF (~ $\phi$ 30 nm) specimens (Figure 1) and the corresponding pore size distribution curves (insert). The Brunauer–Emmett–Teller (BET) surface area calculations gave a high surface area ratio of about 14770 and 7750 m<sup>2</sup>/m<sup>2</sup> for the PF and CF specimens, respectively, with the mesoporous structures attributed to intergranular porosity of the TST coatings instead of the porous structures formed through anodization. That the PF specimen shows larger surface area than the CF specimen may be ascribed to the facts that the former possesses higher porosity than the latter (Figure 1) and that the surface pores in some regions of the latter are partly covered by the TST layer (Figure 1b), even though the latter possesses higher pore density than the former. The significant enhanced surface area of the composite nanostructures can be attributed to the effective combination of the highly nanoporous alumina structures and the rough TST coatings inside the pores, which may be not compatible for currently conventional sol–gel coatings.

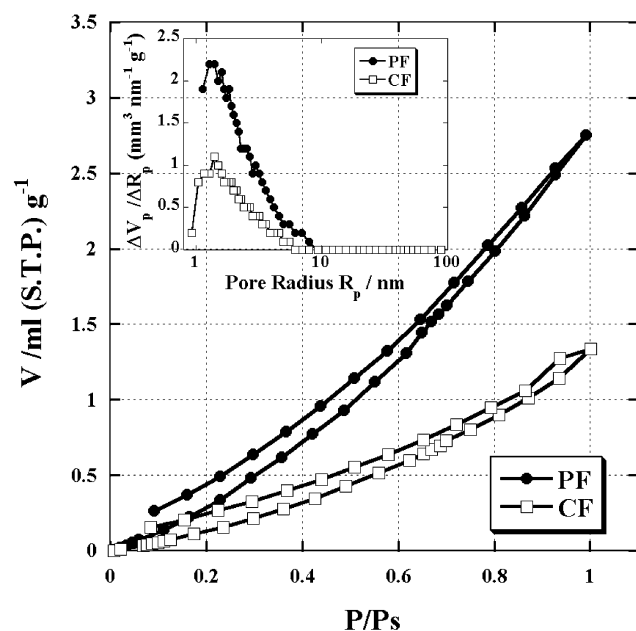


**Figure 3.** Nitrogen adsorption-desorption isotherms of specimens PF (●,  $\phi$ 120 nm) and CF (□,  $\phi$ 30 nm). (Temperature,  $-196^\circ\text{C}$ ; apparatus, BELSORP28A.)

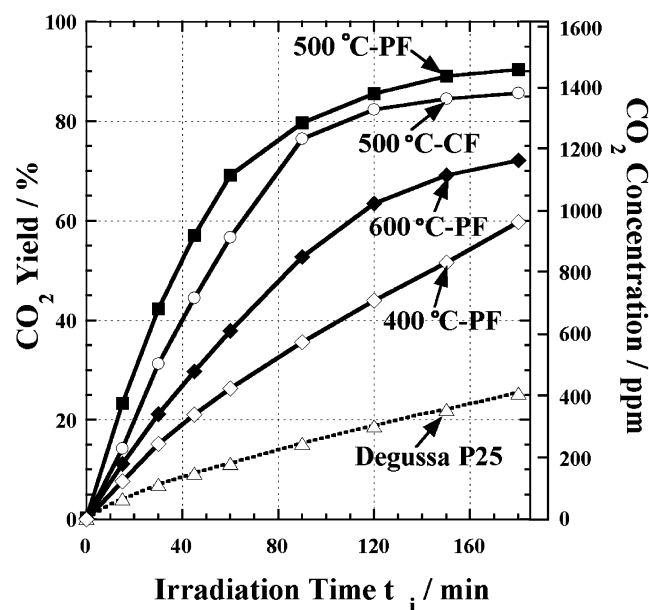


**Figure 4.** Yield and concentration of  $\text{CO}_2$  produced by photodecomposition of acetaldehyde gas on various  $\text{TiO}_2$  samples as a function of the illumination time. Illumination area: porous TST samples,  $1 \times 1 \text{ cm}^2$ ; commercial  $\text{TiO}_2$  powder (Degussa P-25),  $1.3 \text{ cm}^2$  ( $\phi$  1.3 cm, 30 mg).

The photocatalytic activities of the specimens are evaluated in the concentrations of the  $\text{CO}_2$  produced in photodecomposition of acetaldehyde under UV illumination.<sup>19</sup> Figure 4 shows the yields and the concentrations of  $\text{CO}_2$  as a function of illumination time for the porous composite nanostructures and the commercial Degussa P-25  $\text{TiO}_2$  powder. At the each illumination time, the porous composite nanostructures produced much higher  $\text{CO}_2$  yield or concentration than that of the P-25, indicating the enhanced photocatalysis of the formers. For the same morphology (i.e., inner diameter of  $\sim\phi$ 120 nm), the composite nanostructures exhibit the highest result at  $500^\circ\text{C}$ , which may correspond to the crystallization of anatase  $\text{TiO}_2$  and the transition from {004} to {110} reflection (Figure 2).

The result that the PF specimen ( $\sim\phi$ 120 nm) showed higher  $\text{CO}_2$  yield than the CF specimen ( $\sim\phi$ 30 nm) is consistent to the BET result (Figure 3); i.e., larger surface area leads to higher photocatalytic activity. Noticeably, the initial reaction rate ( $R_0$ ) and quantum yields ( $\Phi_{30 \text{ min}} = n_{\text{CO}_2}/n_{\text{photon}}$ )<sup>21</sup> for the PF specimen calcined at  $500^\circ\text{C}$  and P-25 are calculated to be  $3.68 \times 10^{-7} \text{ mol/min}$  and 14.11% and  $0.37 \times 10^{-7} \text{ mol/min}$  and 2.35%, respectively, suggesting that an enhanced photocatalytic activity of 10 times (in  $R_0$ ) or 6 times (in  $\Phi_{30 \text{ min}}$ ) higher than the latter. It should be pointed that within the restrictions of this comparison, the differences in the applicable geometry and light absorbance between the catalysts-powder compared to porous nanostructures and nontransparent<sup>22</sup> to transparent-the data are promising. The enhanced photocatalysis for the porous TST nanostructures compared to the P-25 may be mainly attributed to the combination of the hollow “coral-like” structures with large surface areas and the transparency of the TST<sup>13,14</sup> and/or anodic alumina films;<sup>17,20</sup> i.e., the former ensures the efficient utilization of the whole surface areas in contact with the acetaldehyde gas (surface active sites), and the latter permits the UV light reaching the inside of the porous nanostructures to decompose the acetaldehyde gas there (light absorptive ability). Moreover, the remnant titanium metal underlying the porous nanostructures on glass (Figure 1c,d) may function as a mirror during the photodecomposition test and reflect the UV light into the porous nanostructures, thus enhancing the photocatalytic effect. In addition, it is interesting that the underlying anodic titania layer also endows the specimens a colorful appearance, from yellow, orange, blue, purple, and reddish, to green, varying with anodizing conditions (solution, voltage, time) and heating temperatures. This gives the composite nanostructures another potential application as decorating materials in addition to the purification of our direct environments (air and water).

In summary, we have successfully fabricated a highly porous TST/ $\text{Al}_2\text{O}_3$ / $\text{TiO}_2$  composite nanostructure on a glass substrate with enhanced photocatalysis under UV illumination. Our approach may also be used to achieve or enhance the visible light photocatalysis of the materials by doping some elements such as N,<sup>23</sup> W,<sup>24</sup> or Ta<sup>25</sup> into the  $\text{TiO}_2$ . Furthermore, our fabricating method can be also applied for other substrate materials and be scaled up to large-area products that depend on the sputtering equipments in industry.

**Acknowledgment.** This work is supported by the Japan Millennium Project of “Exploration and Creation of a Catalyst for Removing Harmful Chemical Substances”. The authors thank the Kyodo International Company for assisting the production of sputtered samples. The authors also thank Dr. T. Konishi for assisting the calculation of the porosities of the composite nanostructures.

## References and Notes

- (1) Fujishima, A.; Honda, K. *Nature* **1972**, 238, 37.
- (2) Burnside, S. D.; Shklover, V.; Barbè, C.; Comete, P.; Arendse, F.; Brooks, K.; Grätzel, M. *Chem. Mater.* **1998**, 10, 2419.
- (3) Bischoff, B. L.; Anderson, M. A. *Chem. Mater.* **1995**, 7, 1772.
- (4) Znaidi, L.; Séraphimova, R.; Bocquet, J. F.; Colbeau-Justin, C.; Pommier, C. *Mater. Res. Bull.* **2001**, 36, 811.
- (5) Martin, C. R. *Science* **1994**, 266, 1961.
- (6) Hulteen, J. C.; C. R. Martin. *J. Mater. Chem.* **1997**, 7 (7), 1075.
- (7) Lakshmi, B. B.; Dorhout, P. K.; Martin, C. R. *Chem. Mater.* **1997**, 9, 857.
- (8) Zhang, M.; Bando, Y.; Wada, K. *J. Mater. Sci. Lett.* **2001**, 20, 167.
- (9) Seo, D.-S.; Lee, J.-K.; Kim, H. J. *Crystal Growth*, **2001**, 229, 428.
- (10) Terashima, M.; Inoue, N.; Kashiwabara, S.; Fujimoto, R. *Appl. Surf. Sci.* **2001**, 167, 535.

- (11) Hoyer, P.; Masuda, H. *J. Mater. Sci. Lett.* **1996**, *15*, 1228.
- (12) Ishikawa, Y.; Matsumoto, Y. *Electrochim. Acta* **2001**, *46*, 2819.
- (13) Chu, S. Z.; Wada, K.; Inoue, S.; Todoroki, S. *Chem. Mater.* **2002**, *14* (1), 266.
- (14) Chu, S. Z.; Wada, K.; Inoue, S. *Adv. Mater.* **2002**, *14* (23), 1752.
- (15) Furneaux, R. C.; Rigby, W. R.; Davidson, A. P. *Nature* **1989**, *337*, 147.
- (16) Masuda, H.; Fukuda, K. *Science* **1995**, *268*, 1466.
- (17) Chu, S. Z.; Wada, K.; Inoue, S.; Todoroki, S.; Takahashi, Y. K.; Hono, K. *Chem. Mater.* **2002**, *14* (11), 4595.
- (18) During anodization, the pitting, or the formation of the pores, preferentially initiated in the direction perpendicular to the crystal facet of aluminium and penetrated the thin barrier layer formed in the beginning stage. With the progressing of anodization, the pores developed gradually following the applied electrical field, that is, perpendicular to the substrate.
- (19) The photocatalytic decomposition of acetaldehyde was carried out in a closed circulation system (250 cm<sup>3</sup>) interfaced to a gas chromatograph (Hitachi, G-35A) with a TCD and a PID detector for acetaldehyde and CO<sub>2</sub> analysis, respectively. The reactants are a gaseous mixture of 93.3 kPa CH<sub>3</sub>CHO–He (930 ppm) and 13.3 kPa O<sub>2</sub>. The samples were irradiated from the outside of the reactor by a 200 W Hg–Xe lamp (Hayashi, LA300UV-1,  $\lambda = 365$  nm) with an incident intensity of 50 mW/cm<sup>2</sup>.
- (20) Chu, S. Z.; Wada, K.; Inoue, S.; Todoroki, S. *J. Electrochem. Soc.* **2002**, *149* (7), B321.
- (21) Sopyan, I.; Watanabe, M.; Murasawa, S.; Hashimoto, K.; Fujishima, A. *J. Photochem. Photobiol. A: Chem.* **1996**, *98*, 79.
- (22) The commercial P-25 TiO<sub>2</sub> powder is nontransparent, and the UV light can be absorbed only on the top surface (150–200 nm) of the powdery layer, and thus may limit its photocatalytic performance under the experiment conditions.
- (23) Asahi, A.; Morikawa, T.; Ohwaki, T.; Aoki, K.; Taga, Y. *Science* **2001**, *293*, 269.
- (24) Li, X. Z.; Li, F. B.; Yang, C. L.; Ge, W. K. *J. Photochem. Photobiol. A: Chem.* **2001**, *141* (2–3), 209.
- (25) Zou, Z. G.; Ye, J. H.; Sayama, K.; Arakawa, H. *Nature* **2001**, *414* (12), 625.